ELSEVIER

Coordination Chemistry Reviews
177 (1998) 61–79

COORDINATION CHEMISTRY REVIEWS

Electroabsorption spectroscopy of charge transfer states of transition metal complexes

Bruce S. Brunschwig *, Carol Creutz [1], Norman Sutin [2]

Chemistry Department, Brookhaven National Laboratory, Upton, NY 11973-5000, USA

Received 1 October 1997; accepted 2 July 1998

Contents

Abstract

The use of electroabsorption spectroscopy to determine the dipole-moment changes that occur in the metal-to-ligand, ligand-to-metal, and metal-to-metal charge-transfer transitions in mononuclear and binuclear transition metal complexes is reviewed. The ground-excited state dipole-moment differences are much smaller than expected for the transfer of unit

Abbreviations: 4,4′-bpy, 4,4′-bipyridine; LCAO, linear combination of atomic orbitals; LMCT, ligand-to-metal charge-transfer; MLCT, metal-to-ligand charge-transfer; MMCT, metal-to-metal charge-transfer; phen, 1,10-phenanthroline; py, pyridine; pz, pyrazine; THF, tetrahydrofuran.

* Corresponding author. Tel.: + 1-516-3444332; fax: + 1-516-3445815; e-mail: bsb@bnl.gov.
[1] Tel.: + 1-516-3444301; fax: + 1-516-3447993; e-mail: ccreutz@bnl.gov
[2] Tel.: + 1-516-3444358; fax: + 1-516-3445815; e-mail: sutin@bnl.gov

PII: S0010-8545(98)00188-X

electronic charge between the donor and acceptor centers. The results are discussed in terms of a model in which two factors, electron delocalization and polarization of the acceptor, donor or bridging ligand electrons in response to the changed charge on the metal centers, are considered to be primarily responsible for the relatively small dipole-moment changes. The implications of the results for electronic coupling elements and reorganization energies are also discussed.

Keywords: Charge-transfer transitions; Transition metal complexes; Electroabsorption spectroscopy; Dipole-moment changes; Electronic coupling elements; Solvent reorganization energies

1. Introduction

Charge-transfer transitions result in the displacement of electron density within a molecule or complex. The extent of this charge redistribution can be probed experimentally through studies of (1) electroabsorption (second-order Stark) spectroscopy [1–5], (2) time-resolved microwave [6] and pulsed d.c. [7–9] conductivity changes, (3) microwave absorption measurements [10], (4) the solvent dependence of the charge-transfer band absorption or emission energy [11,12], and (5) Raman and resonance Raman spectroscopy [13,14]. In electroabsorption spectroscopy the effect of an externally applied electric field on the shape of the charge-transfer absorption band is studied. The measurements yield information on the dipole moment and polarizability changes that occur in the charge-transfer transition as well as on the angle between the transition moment and the dipole-moment change. This article reviews the use of electroabsorption spectroscopy to determine the charge redistribution that occurs in the metal-to-ligand charge-transfer (MLCT), ligand-to-metal charge-transfer (LMCT), and metal-to-metal charge-transfer (MMCT) transitions in mononuclear and binuclear transition metal complexes.

The tunability of the $(NH_3)_5RuL$ series (L an aromatic *N*-heterocycle or nitrile) provides a powerful probe of the dependence of the dipole-moment change on the electronic properties of L for the MLCT states of $(NH_3)_5Ru^{II}L$, the LMCT states of $(NH_3)_5Ru^{III}L$, and the MMCT states in ligand-bridged $(NH_3)_5Ru^{II}LRu^{III}(NH_3)_5$ complexes. Boxer and colleagues [2,3] have applied electroabsorption techniques to $(NH_3)_5Ru^{II}L$ where L = pyrazine (pz) and 4,4′-bipyridine (4,4′-bpy) and to their binuclear mixed-valence counterparts and Reimers and Hush have attempted to model the results [15,16]. This work, while revealing significant dipole-moment changes between the ground- and excited-state mononuclear complexes, more surprisingly shows that the changes are appreciably smaller than predicted by widely used models. The measurements were extended to a broader variety of $(NH_3)_5Ru^{II}L$ and $(NH_3)_5Ru^{III}L$ complexes by Shin et al. [4,17] in order to further probe the factors determining the dipole-moment differences between ground- and excited-state systems. More recently, Karki and Hupp [5,18] reported the results of electroabsorption measurements on the MMCT transition in cyanide-bridged binuclear systems. These and other studies are reviewed here.

2. Electroabsorption equations

The changes in molar absorptivity ($\Delta\varepsilon(\nu)$) produced by an applied field arise from changes in both the transition energy and the transition moment. These changes are given by Eqs. (1)–(4) when contributions from the state hyperpolarizabilities ($\boldsymbol{\beta}_g$ and $\boldsymbol{\beta}_e$) and higher order terms are neglected.

$$\boldsymbol{\mu}_g(\boldsymbol{F}) = \boldsymbol{\mu}_g + \boldsymbol{\alpha}_g \cdot \boldsymbol{F} \tag{1}$$

$$\boldsymbol{\mu}_e(\boldsymbol{F}) = \boldsymbol{\mu}_e + \boldsymbol{\alpha}_e \cdot \boldsymbol{F} \tag{2}$$

$$h\Delta\nu = -\Delta\boldsymbol{\mu} \cdot \boldsymbol{F} - \frac{1}{2}\boldsymbol{F} \cdot \Delta\boldsymbol{\alpha} \cdot \boldsymbol{F} \tag{3}$$

$$\boldsymbol{\mu}_{ge}(\boldsymbol{F}) = \boldsymbol{\mu}_{ge} + \boldsymbol{\alpha}_{ge} \cdot \boldsymbol{F} + \frac{1}{2}\boldsymbol{F} \cdot \boldsymbol{\beta}_{ge} \cdot \boldsymbol{F} \tag{4}$$

In the above expressions, $\Delta\boldsymbol{\mu} = (\boldsymbol{\mu}_e - \boldsymbol{\mu}_g)$ and $\Delta\boldsymbol{\alpha} = (\boldsymbol{\alpha}_e - \boldsymbol{\alpha}_g)$ are the changes in dipole moment and polarizability, respectively, between the ground and excited states, $\boldsymbol{F}$ is the applied field, h is Planck's constant, $\boldsymbol{\mu}_{ge}$ is the transition dipole moment, $\boldsymbol{\alpha}_{ge}$ is the transition polarizability tensor and $\boldsymbol{\beta}_{ge}$ is the transition hyperpolarizability tensor.

Electroabsorption measurements on transition-metal complexes have generally been carried out in 50:50 vol% glycerol–water glass at 77 K. The apparatus and techniques are described elsewhere [3,4]. The electroabsorption spectrum is the difference between the absorption spectrum in the presence and absence of the applied electric field ($\sim 10^8$ V m^{-1}). Liptay has derived equations [1,19–21] for the change in the absorption band shape in terms of the zero, first and second derivatives of the zero-field absorption spectrum:

$$\frac{\Delta\varepsilon(\nu)}{\nu} = \left[A_\chi \frac{\varepsilon(\nu)}{\nu} + \frac{B_\chi}{15h} \frac{\partial\left(\frac{\varepsilon(\nu)}{\nu}\right)}{\partial\nu} + \frac{C_\chi}{30h^2} \frac{\partial^2\left(\frac{\varepsilon(\nu)}{\nu}\right)}{\partial\nu^2} \right] \boldsymbol{F}_{int}^2 \tag{5}$$

For a randomly oriented, frozen sample, the following relationships hold:

$$A_\chi = A_1 + (3\cos^2(\chi) - 1)A_2 \tag{6}$$

$$B_\chi = B_1 + (3\cos^2(\chi) - 1)B_2 \tag{7}$$

$$C_\chi = C_1 + (3\cos^2(\chi) - 1)C_2 \tag{8}$$

where χ is the angle between the external (applied) field and the direction of the polarization of the light incident on the sample. The dipole-moment change is generally obtained from the coefficient of the second derivative term:

$$|\Delta\boldsymbol{\mu}| = \sqrt{\frac{C_1}{5}} \tag{9}$$

$$\boldsymbol{m} \cdot \Delta\boldsymbol{\mu} = \sqrt{\frac{C_2}{3} + \frac{C_1}{15}} \tag{10}$$

where $\boldsymbol{m} = \boldsymbol{\mu}_{ge}/|\boldsymbol{\mu}_{ge}|$ is a unit vector oriented along the transition dipole moment. The effect of the orientation of the excited-state dipole on the transition energy is shown in Fig. 1.

The internal field $\boldsymbol{F}_{int}$ which the complex experiences is related to the external field through $\boldsymbol{F}_{int} = f_{int}\boldsymbol{F}_{ext}$ where f_{int} depends on the shape of the solute cavity and on the dielectric constant of the surrounding medium. For a spherical cavity the local field correction f_{int} is $3D_s/(2D_s + 1)$ which corresponds to $f_{int} = 1.0$ to 1.5 for $1.0 < D_s > \infty$. For the 50:50 vol% glycerol–water medium which is often used $f_{int} = 1.33$ [1,4,19–21],while $f_{int} = 1.3$ for frozen THF [5]. (For an ellipsoidal cavity with a long axis appropriate to the M–L length of the pentaammine complexes the value of f_{int} in the glycerol-water medium is 1.2 [4].) A further complication arises from the fact that the pentaammine complexes may be solvated preferentially by water [4,11,12] so that the local dielectric constant could differ from the bulk value. Moreover, f_{int} may vary from one solute to another. Such variation is neglected here.

For the case that both the transition dipole moment and the ground-excited state dipole-moment difference are polarized along the z axis (the M–L bond direction), i.e. $\boldsymbol{m} = [0, 0, 1]$ and within the constraints of a two-state model (the ground and one excited state) the state and transition polarizabilities and hyperpolarizabilities are given by:

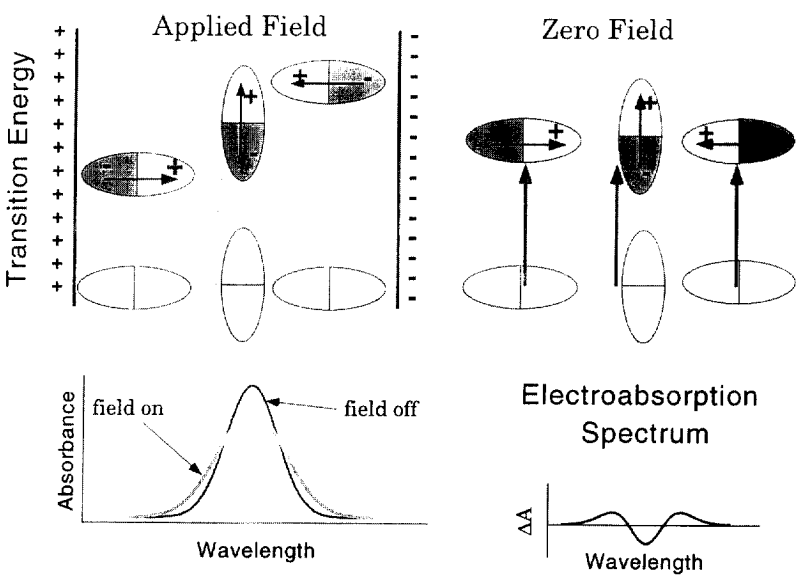

Fig. 1. Pictorial representation of the origin of the electroabsorption spectrum for a molecule that has a dipole moment in its Franck–Condon excited state and none in its ground state. The top of the diagram shows the transition energy in the presence of an applied field and in zero field for three orientations of the molecule. The bottom left shows the effect of the field on the absorption spectrum and the bottom right shows the resulting difference or electroabsorption spectrum.

$$\alpha_g = 2\frac{(\mu_{ge})^2}{(E_e - E_g)} \tag{11}$$

$$\alpha_e = -2\frac{(\mu_{ge})^2}{(E_e - E_g)} \tag{12}$$

$$\Delta\alpha = -4\frac{(\mu_{ge})^2}{(E_e - E_g)} \tag{13}$$

$$\alpha_{ge} = \frac{\mu_{ge}\Delta\mu}{(E_e - E_g)} \tag{14}$$

$$\beta_g = \frac{6\Delta\mu(\mu_{ge})^2}{(E_e - E_g)^2} \tag{15}$$

$$\beta_{ge} = \frac{2\mu_{ge}(\Delta\mu)^2 - 4(\mu_{ge})^3}{(E_e - E_g)^2} \tag{16}$$

A two-state model requires that the polarizabilities of the ground- and excited-states be equal in magnitude but of opposite sign. The latter arises because of the opposite signs of the final-state initial-state energy differences. Further, in the two-state z-polarized model the coefficients in the Liptay expression are related by:

$$A_1 = \tfrac{5}{2}A_2 = \frac{[3(\Delta\mu)^2 - 4(\mu_{ge})^2]}{3(E_e - E_g)^2} \tag{17}$$

$$B_1 = \tfrac{5}{2}B_2 = \frac{10[(\Delta\mu)^2 - (\mu_{ge})^2]}{(E_e - E_g)} \tag{18}$$

$$C_1 = \tfrac{5}{2}C_2 = 5|\Delta\mu|^2 \tag{19}$$

In general, experimental values for B_1/B_2 and C_1/C_2 are close to 2.5, consistent with the one-dimensional, two-state model.

3. Further implications of the one-dimensional, two-state model

To better understand the ground-excited state dipole-moment differences, we consider the implications of the two-state z-polarized model. Our treatment parallels that of Reimers and Hush [15] in most respects. If ψ_a and ψ_b denote the wave functions of the zero-order localized initial and final (for example, metal-centered and ligand-centered) states, their interaction gives rise to two linear combinations (the adiabatic states). The lower energy state, $\psi_g = c_a\psi_a + c_b\psi_b$, corresponds to the ground state and the upper, $\psi_e = c_a\psi_b - c_b\psi_a$, to the excited state (when the overlap integral S_{ab} is neglected, or is zero by construction [22], and the mixing coefficients are normalized, i.e., $c_a^2 + c_b^2 = 1$). The ground-excited state transition occurs at $h\nu = E_e - E_g$ with the transition dipole moment determined from the oscillator strength f_{os} for the transition, Eq. (20) (μ_{ge} in eÅ, energy in cm^{-1}). For a Gaussian-shaped absorption band f_{os} is given by Eq. (21).

$$\mu_{ge} = [f_{os}/(1.08 \times 10^{-5}(E_e - E_g))]^{1/2} \tag{20}$$

$$f_{os} = 4.61 \times 10^{-9} \varepsilon_{max} \Delta\nu_{1/2} \tag{21}$$

Within the two-state model,

$$\mu_{ge} = c_a c_b (\mu_b - \mu_a) \tag{22}$$

where $(\mu_b - \mu_a) = er_{ab}$ is the difference between the dipole-moments of the diabatic (localized) states, r_{ab} is the effective electron-transfer distance, and the transition dipole moment between the localized states (μ_{ab}) is assumed to be zero [4,22,23]. As a result of the interaction of the localized states, the charge transferred in the optical transition is decreased from e to $(1 - 2c_b^2)e$ and the measured dipole-moment change $\Delta\mu$ and the dipole-moment difference between the diabatic states $(\mu_b - \mu_a)$ are thus related by [4,22]:

$$\Delta\mu = (\mu_e - \mu_g) = (1 - 2c_b^2)(\mu_b - \mu_a) \tag{23}$$

In other words, electron delocalization reduces the ground-excited state dipole-moment difference by $2c_b^2 er_{ab} = 2c_b^2|(\mu_b - \mu_a)|$. Further, the ground-excited state dipole-moment difference and the transition dipole moment are related by:

$$\Delta\mu = \left(\frac{c_a^2 - c_b^2}{c_a c_b}\right)\mu_{ge} \tag{24}$$

The diabatic dipole-moment difference, an important parameter in the electronic coupling and reorganization energy expressions discussed below, can thus be calculated from purely experimental quantities [15,23]:

$$(\mu_b - \mu_a) = [(\Delta\mu)^2 + 4(\mu_{ge})^2]^{1/2} \tag{25}$$

(an alternative way of stating the above relationships is to recall that the off-diagonal matrix elements μ_{ab} of the diabatic dipole-moment matrix are all zero. The matrix of the c_i coefficients, C, transforms the diabatic to the adiabatic wave functions. C also diagonalizes the Hamiltonian and converts the diagonal diabatic dipole-moment matrix to the nondiagonal adiabatic dipole-moment matrix through a similarity transformation.)

The molecular and state properties are readily related through the magnitude of c_b^2. In general, c_b^2 is a function of the energy differences between the diabatic states and their symmetry and spatial properties. It can be calculated from experimental quantities using Eq. (26) (which follows from Eq. (23)) with $(\mu_b - \mu_a)$ given by Eq. (25) [17,23].

$$c_b^2 = \frac{1}{2}\left(1 - \frac{\Delta\mu}{\mu_b - \mu_a}\right) \tag{26}$$

It is apparent from the above expressions that $\Delta\mu \to (\mu_b - \mu_a)$ and $\mu_{ge} \to 0$ as the system becomes more localized, i.e. as $c_b^2 \to 0$, and that $\Delta\mu \to 0$ and $(\mu_b - \mu_a) \to 2\mu_{ge}$ as the system becomes delocalized, i.e. as $c_b^2 \to 1/2$. The charges and distances implicated in the diabatic and adiabatic dipole-moment changes in MLCT and LMCT transitions are summarized in Table 1.

Table 1
Dipole-moment changes in MLCT and LMCT transitions

Description	Charge transferred	Effective distance[b]
Primitive dipole-moment change[a]	e	r^0
Diabatic dipole-moment difference ($\mu_b - \mu_a$)	e	r_{ab}
Contribution from ground-state delocalization	$2c_b^2 e$	r_{ab}
Adiabatic dipole-moment change ($\mu_e - \mu_g$)	$(1-2c_b^2)e$	r_{ab}

[a] The primitive model neglects the dipole-moment change resulting from the polarization of the metal and ligand valence electrons: r^0 is the distance separating the localized donor and (reduced) acceptor charge centroids and can be viewed as the distance between the average positions of the transferring electron.

[b] The effective electron transfer distance $r_{ab} \equiv |(\mu_b - \mu_a)/e|$ is the distance over which a single electron would need to be transferred if its displacement were solely responsible for the dipole-moment difference between the localized states. It is usually much less than r^0 because of valence electron repolarization.

4. Comparisons of experimental dipole-moment and polarizability changes with the two-state model predictions

Dipole-moment changes determined by electroabsorption spectroscopy for MLCT, LMCT and MMCT transitions in transition metal complexes are summarized in Table 2. As discussed previously [3,4,17], the $\Delta\mu$ values are much smaller than those obtained from a primitive model in which an electron is assumed to transfer between the donor and acceptor centers with the remaining electrons frozen. Values of $(\mu_b - \mu_a)$ calculated from Eq. (25) and of c_b^2 calculated from Eq. (26) are also included in Table 2.

4.1. Metal-to-ligand and ligand-to-metal charge transfer transitions

In a recent treatment of MLCT and LMCT transitions [4,17] two factors, electron delocalization and polarization of the ligand electrons, are considered to be primarily responsible for the relatively small ground-excited state dipole-moment changes. These will be discussed in turn.

Because of π-backbonding for the M(II) and π-bonding for the M(III) complexes, less than unit electron charge is transferred from the donor to the acceptor in the optical transition. Thus, the negligible $\Delta\mu$ values for the high-energy transitions in $[(NH_3)_5Ru^{II}pzH]^{3+}$ and $[(NH_3)_5Ru^{II}pzCH_3]^{3+}$ (Table 2) are correlated with essentially complete delocalization of the orbitals involved ($c_b^2 \approx 0.5$). As discussed elsewhere [12,24,25], the high-energy transitions in the pyrazinium complexes are best described as bonding-to-antibonding, rather than as MLCT, an assignment consistent with the solvent independence of the high-energy band. Similar considerations apply to the high-energy transition in $[(NH_3)_5Os^{II}pzCH_3]^{3+}$, which has some LMCT character with $c_b^2 = 0.27$ and $\Delta\mu = 1.1$ eÅ. (The assignment of the high- and low-energy transitions of the Os(II) complex as LMCT and MLCT, respectively, is based on the solvent dependence of the transitions and their

Table 2
Dipole-moment changes and electronic coupling elements in glycerol–water glass at 77 K

Complex	$\lvert\mu_{ge}\rvert$[a] (eÅ)	$\lvert\Delta\mu\rvert$[b] (eÅ)	$\lvert(\mu_b-\mu_a)\rvert$ (eÅ)	c_b^2[c]	H_{ab}[d] (kK)	Ref.
MLCT						
$[(NH_3)_5Ru^{II}py]^{2+}$	0.8	0.7	1.7	0.30	10.5	[4]
$[(NH_3)_5Ru^{II}py\text{–}4\text{-}NH_2]^{2+}$	0.8	1.2	2.0	0.19	10.1	[4]
$[(NH_3)_5Ru^{II}py\text{–}4\text{-}COO^-]^{+}$	1.0	1.4	2.4	0.20	8.0	[4]
$[(NH_3)_5Ru^{II}py\text{–}4\text{-}COOH]^{2+}$	1.0	1.2	2.3	0.24	8.0	[4]
$[(NH_3)_5Ru^{II}py\text{–}4\text{-}CONH_2]^{2+}$	1.0	1.9	2.7	0.15	6.8	[4]
$[(NH_3)_5Ru^{II}py\text{–}3,5\text{-}(COO^-)_2]$	0.7	1.6	2.1	0.12	7.0	[4]
$[(NH_3)_5Ru^{II}py\text{–}3,5\text{-}(COOH)_2]^{2+}$	0.7	1.5	2.0	0.13	7.0	[4]
$[(NH_3)_5Ru^{II}pz]^{2+}$	1.0	0.7	2.1	0.32	9.4	[4]
	1.0	0.8	2.2	0.32	9.1	[3]
$[(NH_3)_5Ru^{II}pzH^+]^{3+}$ (h)	1.0	≤ 0.4	2.1[e]	0.5[e]	9.3[e]	[4]
$[(NH_3)_5Ru^{II}pzCH_3^+]^{3+}$ (h)	1.2	≤ 0.4	2.3[e]	0.5[e]	9.3[e]	[4]
$[(NH_3)_5Ru^{II}pzCH_3^+]^{3+}$ (l)	0.2	1.0	1.0	0.02	1.6	[4]
$[(NH_3)_5Ru^{II}4,4'\text{–}bpy]^{2+}$	1.0	2.7	3.4	0.09	5.5	[4]
	1.0	2.5	3.2	0.11	5.9	[3]
$[(NH_3)_5Ru^{II}4,4'\text{-}bpyH^+]^{3+}$	1.1	3.5	4.3	0.07	4.2	[4]
	1.1	3.1	3.8	0.09	4.6	[3]
$[(NH_3)_5Ru^{II}4\text{-}NCpy]^{2+}$	0.9	2.5	3.1	0.09	6.3	[4]
$[(NH_3)_5Ru^{II}4\text{-}NCpyH^+]^{3+}$	1.1	1.8	2.8	0.18	6.9	[4]
$[(NH_3)_5Ru^{II}NCph]^{2+}$	1.0	1.8	2.6	0.16	9.2	[4]
$[(NH_3)_5Ru^{II}1,4\text{-}NCphCN]^{2+}$	1.1	2.0	3.0	0.17	8.0	[4]
$[(NH_3)_5Os^{II}pzCH_3^+]^{3+}$ (l)	0.3	0.6	0.9	0.16	3.1	[4]
LMCT						
$[(NH_3)_5Ru^{III}py\text{–}4\text{-}NH_2]^{3+}$	0.5	2.7	2.9	0.03	3.4	[4]
$[(NH_3)_5Ru^{III}py\text{–}4\text{-}OH]^{3+}$	0.4	2.5	2.7	0.02	3.1	[4]
$[(NH_3)_5Ru^{III}py\text{–}4\text{-}N(CH_3)_2]^{3+}$	0.4	2.7	2.8	0.02	2.6	[4]
$[(NH_3)_5Ru^{III}NCph\text{–}4\text{-}N(CH_3)_2]^{3+}$	0.4	5.8	5.9	0.005	1.0	[4]
$[(NH_3)_5Os^{II}pzCH_3^+]^{3+}$ (h)	1.0	1.1	2.4	0.27	10.2	[4]

Table 2 (*Continued*)

Complex	$\lvert\boldsymbol{\mu}_{ge}\rvert$[a] (eÅ)	$\lvert\Delta\boldsymbol{\mu}\rvert$[b] (eÅ)	$\lvert(\boldsymbol{\mu}_b-\boldsymbol{\mu}_a)\rvert$ (eÅ)	c_b^2[c]	H_{ab}[d] (kK)	Ref.
MMCT						
$[(NH_3)_5Ru^{II}$–pz–$Ru^{III}(NH_3)_5]^{5+}$	0.7	0.1	1.3	0.46	2.2	[3]
$[(NH_3)_5Ru^{II}$–4,4′-bpy–$Ru^{III}(NH_3)_5]^{5+}$	0.5	4.5	4.6	0.01	0.9	[3]
$[(CN)_5Fe^{II}$–CN–$Os^{III}(NH_3)_5]^-$	0.4	2.6	2.7	0.02	2.6	[5]
$[(CN)_5Os^{II}$–CN–$Ru^{III}(NH_3)_5]^-$ (∥)	0.7[f]	2.8	3.1	0.05	2.9[f]	[18]
$[(CN)_5Os^{II}$–CN–$Ru^{III}(NH_3)_5]$ (⊥)	0.4[f]	4.0	4.1	0.01	1.4[f]	[18]

[a] Transition dipole moment calculated from Eq. (20).

[b] Dipole-moment difference calculated from $f_{int}\lvert\Delta\boldsymbol{\mu}\rvert$ using $f_{int}=1.33$.

[c] Degree of delocalization calculated from Eq. (26). Note that c_b is the coefficient of the higher energy orbital in the lowest energy LCAO expression, i.e., the coefficient of $L\pi^*$ for the MLCT and of $d\pi$ for the LMCT transitions considered here. See also Appendix A.

[d] Electronic coupling element calculated from Eqs. (30a) and (30b).

[e] Calculations based on $\lvert\Delta\boldsymbol{\mu}\rvert=0.2$ eÅ.

[f] Oscillator strengths estimated from spectral data in [40,18].

dependence on the L/L^- reduction potential [12].) In contrast to the high-energy transition, the low-energy band in $[(NH_3)_5Ru^{II}pzCH_3]^{3+}$ shows a normal MLCT solvent dependence with a dipole moment change slightly larger than that for the pyridine and pyrazine complexes. For this transition $c_b^2 = 0.02$, which is much less than c_b^2 for the other MLCT transitions. This arises because the low-energy transition in $[(NH_3)_5Ru^{II}pzCH_3]^{3+}$ originates from a t_{2g}-type d_δ orbital that interacts only weakly with the ligand π^* orbital due to small spatial overlap [25]. At the other extreme, the dipole-moment change in the LMCT transition in $[(NH_3)_5Ru^{III}$–NCph–4-$N(CH_3)_2]^{3+}$ is very large, again consistent with a highly localized description ($c_b^2 < 0.01$). The dipole-moment change in the MLCT transition in $Ru(phen)_3^{2+}$ is 1.4 eÅ [26], very similar to the value reported for $Ru(bpy)_3^{2+}$ [27]. Formation of the triplet MLCT state of $Ru(phen)_3^{2+}$ is also accompanied by a similar dipole-moment change [26]. The electroabsorption results are inconsistent with time-resolved resonance Raman studies which suggest that the MLCT excited state of $Ru(phen)_3^{2+}$, unlike that of $Ru(bpy)_3^{2+}$, is delocalized [28].

The second major factor determining the dipole-moment change is the displacement of the ligand valence electrons as a result of the changed charge on the metal center. In an MLCT transition, the charge on the metal center is increased by the transfer of an electron from the metal to the ligand. The higher charge causes the ligand electron distribution to shift toward the metal center, resulting in a dipole-moment change opposing the change produced by the transferring electron. Analogous considerations apply to an LMCT transition. Within this framework, the dipole-moment difference between the localized ground and excited states in MLCT and LMCT transitions is given by Eq. (27), where n is the number of valence electrons in L (for example, 30 for pyridine), r^0 is the distance between the metal center and the negative charge center of the localized ligand, and Δr is the displacement of the negative charge center of the ligand as a result of the altered charge on the metal center (Fig. 2). Note that r^0 and Δr have opposite signs.

$$(\boldsymbol{\mu}_b - \boldsymbol{\mu}_a) \approx er^0 + ne\Delta r \tag{27}$$

The first term on the RHS is the product of a unit charge and the distance between the metal center and the negative charge center of the ligand. This term can be viewed as the dipole-moment change due to the transferring electron [4]. Although there is only a very small displacement of the negative charge center of the ligand, i.e. $|\Delta r| \ll |r^0|$, the second term is still significant because n is large. Thus the ground-excited state dipole-moment difference is generally much less than the dipole-moment change associated with the transferring electron because an opposing dipole-moment change is produced by the displacement (polarization) of the remaining valence electrons.

The effect of valence electron polarization has been estimated by using an INDO-SCF method [29] to determine the shift of the center of the ligand valence electrons upon MLCT and LMCT excitation [17]. This approach does rationalize the relatively low $(\boldsymbol{\mu}_b - \boldsymbol{\mu}_a)$ values for the pentaammineruthenium(II) and (III) complexes [4]. The calculations show that the valence electron repolarization contribution is larger for MLCT transitions, accounting for their lower $(\boldsymbol{\mu}_b - \boldsymbol{\mu}_a)$ values for a given L [17].

The ground-excited state polarizability differences calculated from the two-state Eq. (13) range from $-(3.9 \text{ to } 1.1) \times 10^{-39}$ C m^2 V^{-1}. On the other hand, the values estimated from the *B* coefficients of the electroabsorption spectra vary from $(-1 \text{ to } +21) \times 10^{-39}$ C m^2 V^{-1} [4]. The most negative $\Delta\alpha$ values are for the Ru(II) and Os(II) complexes with L = pz, pzH$^+$ and pzCH$_3^+$. Evidently, the polarizability differences cannot readily be rationalized within a two-state model and it is necessary to include higher excited states. This is particularly true for excited-state polarizabilities. The effect of the permanent dipoles of the NH_3 ligands on the ground-excited state dipole-moment changes has also been considered [4,15]. The effects are difficult to model because of the uncertainty regarding the magnitudes, and even the signs, of the ground-excited state polarizability differences. An ab initio treatment of the MLCT dipole-moment changes in $(NH_3)_5Ru^{II}L$ complexes with L = pz, pzH$^+$ and py has been published recently [30,31]. The results are encouraging.

4.2. Metal-to-metal charge transfer transitions

Although the electroabsorption spectrum of $[(NH_3)_5Ru^{II}-pz-Ru^{III}(NH_3)_5]^{5+}$ is complicated [3], the small dipole-moment change in the MMCT transition is indicative of essentially complete electron delocalization ($c_b^2 \approx 1/2$). The same conclusion has been reached from other studies of the pyrazine-bridged complex

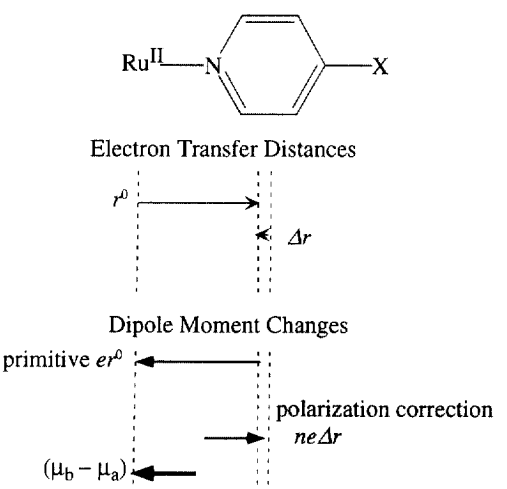

Fig. 2. Illustration of the contributions to the diabatic dipole-moment change in the MLCT transitions in $(NH_3)_5Ru^{II}py-X$. The top section show the primitive one-electron transfer distance, r^0, and the difference in the position of the center of negative charge on the ligand in the ground and excited states of the complex, Δr (this distance is exaggerated for clarity). The bottom section shows the two contributions to the diabatic dipole-moment change ($\mu_b - \mu_a$): er^0 is the primitive dipole-moment change due to the transfer of one electron from the Ru center to the center of negative charge on the ligand and $ne\Delta r$ is the opposing dipole-moment change produced by the shift in the negative charge center of the ligand as a result of the increased charge on the metal center.

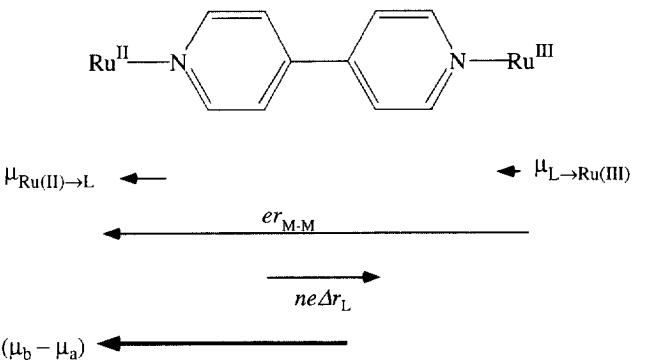

Fig. 3. Illustration of the contributions to the diabatic dipole-moment change in the MMCT transition in $[(NH_3)_5Ru^{II}$–4,4′-bpy–$Ru^{III}(NH_3)_5]^{5+}$. er_{M-M} is the primitive dipole-moment change due to the transfer of an electron between the Ru centers, $ne\Delta r_L$ is the dipole-moment reduction due to the polarization of the electrons of the bridging ligand, $\mu_{Ru(II)\rightarrow L}$ and $\mu_{L\rightarrow Ru(III)}$ are dipoles resulting from metal-to-ligand and ligand-to-metal electron delocalization, respectively, and $(\mu_b - \mu_a)$ is the diabatic dipole-moment change for the MMCT transition.

[32]. By contrast, the dipole-moment change in the MMCT transition in $[(NH_3)_5Ru^{II}$–4,4′-bpy–$Ru^{III}(NH_3)_5]^{5+}$ is larger than any of the MLCT values in Table 1 and is consistent with a localized structure ($c_b^2 \approx 0.01$), with the dipole-moment correction for metal-metal delocalization amounting to only about 0.1 eÅ. The value of $(\mu_b - \mu_a)$ for the MMCT transition in the bipyridine-bridged complex is 4.6 eÅ, slightly larger than the diabatic dipole-moment difference in $[(NH_3)_5Ru^{II}$–4,4′-bpyH$^+]^{3+}$. For comparison, the metal–metal separation in the binuclear complex is 11.3 Å [32]. There is no metal-to-ligand or ligand-to-metal electron delocalization in the diabatic states for MLCT and LMCT transitions and Eq. (25) allows for the delocalization in the adiabatic charge-transfer states. For MMCT transitions, Eq. (25) only corrects for the metal-to-metal delocalization, which is small for weakly coupled binuclear systems. However, metal-to-ligand and ligand-to-metal electron delocalization is present in the diabatic states for MMCT transitions and this interaction will change the effective metal-to-metal charge-transfer distance. Thus, in terms of the present model, the factors primarily determining the dipole-moment change in the MMCT transition in $[(NH_3)_5Ru^{II}$–4,4′-bpy–$Ru^{III}(NH_3)_5]^{5+}$ are metal–ligand electron delocalization and repolarization of the ligand valence electrons. Accordingly, the dipole-moment change in the MMCT transition is given by:

$$(\mu_e - \mu_g) \cong (\mu_b - \mu_a) = er_{M-M} - 2(|\mu_{Ru(II)\rightarrow L}| + |\mu_{L\rightarrow Ru(III)}|) - ne|\Delta r_L| \qquad (28)$$

where r_{M-M} is the Ru–Ru separation in the binuclear complex, $2|\mu_{Ru(II)\rightarrow L}|$ and $2|\mu_{L\rightarrow Ru(III)}|$ are the contributions to the dipole-moment change from metal-to-ligand and ligand-to-metal delocalization, respectively (the factor 2 arises because there are two ruthenium centers), and $|\Delta r_L|$ is the displacement of the valence electrons of the bridging ligand in the MMCT transition (Fig. 3).

We model the metal-ligand delocalization in the binuclear complex by the delocalization obtaining in the corresponding mononuclear complexes. The difference between the $(\mu_b - \mu_a)$ and $\Delta\mu$ values for MLCT in $[(NH_3)_5Ru^{II}-4,4'\text{-}bpyH^+]^{3+}$ indicates that the ground-state Ru(II)-to-ligand delocalization reduces the dipole-moment change by 0.8 eÅ $(2c_b^2|(\mu_b - \mu_a)|$, see Appendix A). The corresponding difference for the LMCT transitions in the $(NH_3)_5Ru^{III}py-X$ complexes shows the effect of the ground-state ligand-to-Ru(III) delocalization to be much less, amounting to only about 0.1 eÅ $(c_b^2|(\mu_b - \mu_a)|$, Appendix A). Assuming a similar degree of interaction of the metal centers with the bridging ligand in the binuclear complex (a reasonable assumption since the MLCT transition dipole moments for the mononuclear and binuclear complexes differ by only $\sim 5\%$ [33–35]), metal–ligand delocalization will lower the dipole-moment change for the MMCT transition in $[(NH_3)_5Ru^{II}-4,4'\text{-}bpy-Ru^{III}(NH_3)_5]^{5+}$ by about $2 \times (0.8 + 0.1) \approx 2$ eÅ. For comparison, ZINDO calculations of the shift of the charge centroids of the three $4d_\pi$-type spin orbitals in $[(NH_3)_5Ru^{II}-4,4'\text{-}bpy-Ru^{III}(NH_3)_5]^{5+}$ indicate a somewhat larger degree of delocalization. With the Ru(II) and Ru(III) located at -5.65 and $+5.65$ Å, respectively, the centroids of the doubly and singly occupied $4d_\pi$ orbitals are found at -4.80 and $+5.42$ Å. These shifts translate to a 2.9 eÅ decrease in the MMCT dipole-moment change.

The repolarization of the bipyridine valence electrons resulting from the change in the metal charges can be estimated from a ZINDO calculation in which 2+ and 3+ point charges are placed 2.0 Å from the N atoms of the bipyridine to simulate the metal charges in the mixed-valence complex. These calculations indicate a contribution of ~ 2.8 eÅ from ligand electron repolarization. The effects of the metal–ligand electron delocalization and the bipyridine valence electron repolarization thus yield a $(\mu_b - \mu_a)$ of ~ 6 eÅ, close to the 4.6 eÅ observed for the MMCT transition in the 4,4′-bipyridine-bridged mixed-valence complex.

The dipole-moment change in $[(NC)_5Fe^{II}-CN-Os^{III}(NH_3)_5]^-$ corresponds to only about half the Fe–Os separation [5]. Similar results were found for the dipole-moment change in $[(NC)_5Os^{II}-CN-Ru^{III}(NH_3)_5]^-$ [18]. As a consequence of the stronger spin–orbit coupling and greater d orbital extension obtaining in the latter binuclear complex, charge transfer from the d_δ orbital is less unfavorable and two MMCT transitions are seen, a lower energy (d_π, parallel) transition with a dipole-moment change of 2.8 eÅ and a higher energy, less intense (d_δ, perpendicular) transition with a dipole-moment change of 4.0 eÅ. As expected from the naive model, the d_δ orbital is less mixed with the bridging ligand orbitals and the transition from the d_δ orbital features the larger dipole-moment change. However, delocalization is not sufficient to account for the small dipole-moment changes and it is again necessary to invoke valence electron repolarization to rationalize the results [18]. Finally, when the donor and acceptor sites are symmetrical and their electronic coupling weak, as in linked iron polypyridyl complexes, the metal–metal separation approximates closely the effective charge-transfer distance [36]. The effects of spin–orbit mixing also need to be more explicitly considered.

5. Electronic coupling elements

The electronic matrix element coupling the two diabatic states can be evaluated from spectroscopic properties utilizing the Mulliken–Hush expression. The latter expression is usually cast in terms of r_{ab}, the donor–acceptor separation. However, as discussed elsewhere [22,23], $(\mu_b - \mu_a)$, the difference between the dipole moments of the diabatic states, is the more fundamental quantity, and indeed, in its original derivation [37], the electronic coupling element H_{ab} is expressed in terms of $(\mu_b - \mu_a)$, as shown in Eq. (29):

$$|H_{ab}| = \left|\frac{\bar{\nu}_{max}\mu_{ge}}{\mu_a - \mu_b}\right| \tag{29}$$

Since the diabatic dipole-moment difference is related to the transition moment and measured dipole-moment change by Eq. (25), $(\mu_b - \mu_a)$ is readily derivable from measurable quantities. Eq. (29) is applicable to both class II (localized) and class III (delocalized) systems of the Robin and Day classification [22].

The H_{ab} values in Table 2 are generally 30–50% lower than the electronic coupling values presented earlier [22]. The latter were based on r^0 rather than on r_{ab} values. As is evident from Table 2, the metal–ligand coupling elements derived from the d_π MLCT transitions in the $(NH_3)_5Ru^{II}$py-X complexes range from $(7–10.5) \times 10^3$ cm^{-1} while those for the LMCT transitions in the $(NH_3)_5Ru^{III}$py–X complexes vary from $(2.6–3.4) \times 10^3$ cm^{-1}. For purposes of comparison, it is necessary to divide the Ru(II) values by $\sqrt{2}$ to allow for the two Ru(II) spin configurations (deriving from excitation of either d_π electron). Despite this, the Ru(II) complexes still feature larger coupling elements. In terms of Eq. (29), the larger H_{ab} values for the Ru(II) complexes derive primarily from the larger oscillator strengths for the MLCT transitions and their smaller dipole-moment changes.

The metal–ligand coupling elements enter into superexchange expressions for the metal–metal coupling elements H_{MM} in weakly coupled ligand-bridged mixed-valence systems. In MMCT transitions in diruthenium decaammine systems in which the Ru–Ru coupling is provided by mixing with an MLCT state, H_{MM} is given by Eqs. (30a) and (30b) where H_{ML} is the metal–ligand coupling element for $(NH_3)_5Ru^{II}L$ at the Ru^{II}–N equilibrium configuration, $H_{M'L}$ is the corresponding quantity for a $(NH_3)_5Ru^{II}L$ at the Ru^{III}–N geometry, and ΔE_{ML} is the effective metal–ligand energy gap [22].

$$H_{MM} = \frac{H_{ML}H_{M'L}}{2\Delta E_{ML}} \tag{30a}$$

$$\frac{1}{\Delta E_{ML}} = \frac{1}{2}\left(\frac{1}{\Delta E_{MLCT}} - \frac{1}{\Delta E_{MLCT} - \Delta E_{MMCT}}\right) \tag{30b}$$

Recent calculations have shown that H_{ML} and $H_{M'L}$ for $(NH_3)_5Ru^{II}L$ complexes do not differ significantly [38], and the elements will be assumed to be equal for the systems considered here. The value of the metal-metal coupling element for $[(NH_3)_5Ru^{II}–4,4'\text{-bpy}–Ru^{III}(NH_3)_5]^{5+}$, calculated from Eqs. (30a) and (30b) with

$H_{ML} = H_{M'L} = 4.4 \times 10^3$ cm^{-1} and $\Delta E_{ML} = 12.7 \times 10^3$ cm^{-1} [22], is 0.8×10^3 cm^{-1}, in satisfactory agreement with the value of 0.9×10^3 cm^{-1} calculated from the Mulliken–Hush expression. This comparison shows the utility of the superexchange formalism and Eqs. (30a) and (30b).

6. Solvent reorganization energies

The charge transferred and the electron-transfer distance also enter into expressions for the solvent contribution to the charge-transfer barrier. In the notation used here, the solvent reorganization energy for electron transfer between two redox sites centrally located in two noninterpenetrating spheres, modified for electron delocalization is:

$$\lambda_{mod} = ((1 - 2c_b^2)e)^2\left(\frac{1}{2r_a} + \frac{1}{2r_b} - \frac{1}{r_{ab}}\right)\left(\frac{1}{D_{op}} - \frac{1}{D_s}\right) \tag{31}$$

where r_a and r_b are the radii of the sites and D_{op} and D_s are the optical and static dielectric constants of the surrounding medium, respectively. For electron transfer between two sites located symmetrically on the major axis of an ellipsoidal molecule, the solvent reorganization energy is given by:

$$\lambda_{mod} = \frac{((1 - 2c_b^2)e)^2}{R}\left(\frac{1}{D_{op}} - \frac{1}{D_s}\right)SF_1 \tag{32}$$

where R is the distance between the foci of the ellipsoid and it has been assumed that the internal dielectric constant of the ellipsoid is equal to the optical dielectric constant of the medium [39]. The shape factor SF_1 is a function of r_{ab}, R, the lengths of the major and minor axes of the ellipsoid, and the dielectric constants of the surrounding medium. For the special case where the donor and acceptor sites are located at the foci of the ellipsoid and certain image effects are neglected, the solvent reorganization energy becomes:

$$\lambda_{mod} = \left(\frac{(\Delta\mu)^2}{2AB^2}\right)\left(\frac{1}{D_{op}} - \frac{1}{D_s}\right)SF_2 \tag{33}$$

where $2A$ and $2B$ are the lengths of the major and two minor axes of the ellipsoid, respectively, and SF_2 is a function only of A and B [39].

The above expressions yield lower reorganization energies than their classical counterparts in which the donor-acceptor separation is approximated by the geometrical center-to-center distance and delocalization is neglected. Since the solvent reorganization energy is proportional to the square of the charge transferred, the effect of electron delocalization on the reorganization energy can be quite large.

As an illustration of the effect of the distance change we consider the MMCT transition in the 4,4′-bpy-bridged diruthenium mixed-valence complex. The two-sphere expression, Eq. (31), is restricted to systems for which $r_{ab} \geq (r_a + r_b)$, a condition not satisfied by the binuclear complex. With the assumption that the two spheres are in contact ($r_{ab} = 2r_a = 2r_b = 7.94$ Å) and $c_b = 0$, Eq. (31) yields $\lambda_{out} = 23.0$

kcal mol^{-1}. This value, together with $\lambda_{in} = 4.1$ and $\lambda_{so} = 3.6$ kcal mol^{-1} [39], yields 30.7 kcal mol^{-1} for the MMCT transition energy, in good agreement with the observed value of 27.8 kcal mol^{-1} ($\lambda_{out} = 0.1$ kcal mol^{-1}) [32]. Despite this good agreement, the effective charge transfer distance implicated by the dipole-moment change (4.6 Å) is less than the close-contact r_{ab} value used in the calculation. The shape of the molecule and the relative short charge-transfer distance suggest that the binuclear complex may be more appropriately modeled by an ellipsoidal cavity. For $r_{ab} = 4.6$, 7.94 and 11.3 Å, Eq. (32) with the constant-volume assumption [39] yields $\lambda_{out} = 13.7$, 27.9, and 42.8 kcal mol^{-1}, respectively. The minimum-enclosing-volume assumption for the ellipsoidal cavity yields lower solvent reorganization energies (Fig. 4). The effect of changing the charge transfer distance is thus quite dramatic, with the constant-volume condition for the ellipsoidal cavity together with r_{ab} values in the range 5.5–7.2 Å ($r_{ab}/2A = 0.3$–0.4) yielding reasonable agreement with the experimental λ_{out} value.

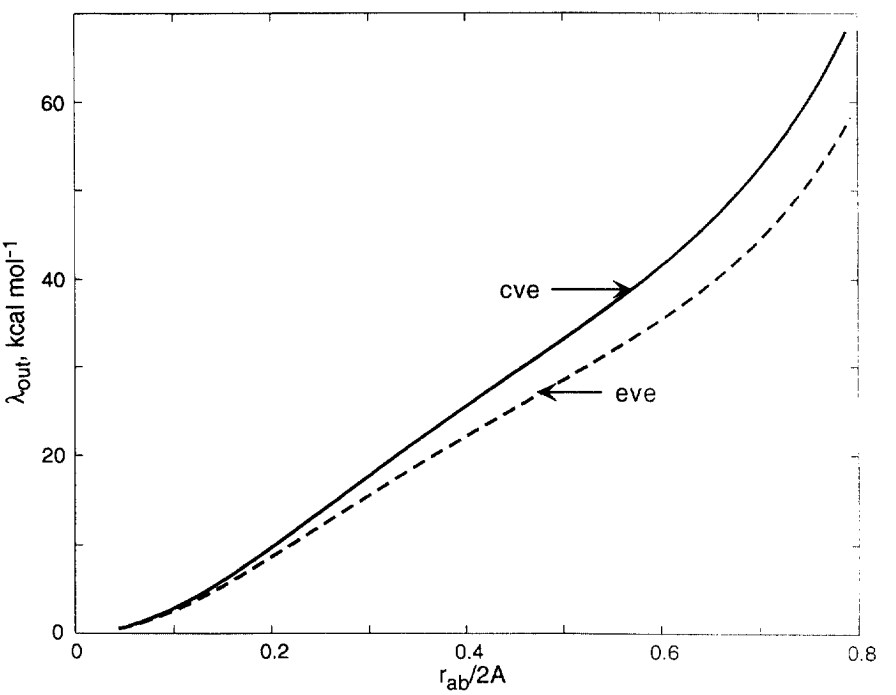

Fig. 4. Plot of the outer-shell reorganization energy versus $r_{ab}/2A$ calculated using the ellipsoidal cavity model. The curves are constructed assuming that the charge transfer sites are located symmetrically a distance r_{ab} apart on the major axis of the ellipsoid: cve and eve represent the constant-volume ellipsoid and minimum-enclosing-volume ellipsoid models, respectively [39]. The cve assumption yields an ellipsoid with major axis ($2A$), minor axes ($2B$), and interfocal length (R) equal to 18.4, 7.10 and 17.0 Å, respectively, while the corresponding eve axes and interfocal length are 22.7, 8.42, and 10.54 Å. The cve model constructs a cavity with a volume equal to that of $[(NH_3)_5Ru^{II}$–4,4′-bpy–$Ru^{III}(NH_3)_5]^{5+}$ idealized as two spheres of effective radius 3.87 Å. The major axis of the ellipsoid just encloses the two axial ammines which extend 3.55 Å from the metal centers. The eve model constructs the smallest ellipsoidal cavity that completely encloses the binuclear complex. The Ru–Ru separation in the complex is 11.3 Å.

Finally, the delocalization-corrected reorganization expressions should be used with caution [41]. For example, the energy of the optically induced charge transfer in a symmetrical double well system, ν_{max}, is independent of the degree of delocalization [22]. This arises because an additional term in ν_{max} cancels the delocalization correction to λ_{out} and λ_{in}. Detailed energy expressions that illustrate the effect of delocalization are available [41].

7. Conclusions

Data from absorption (transition dipole moment) and electroabsorption (dipole-moment change) spectroscopy can be combined with a two-state model to give estimates of the degree of mixing of the (noninteracting) diabatic states, the dipole moment difference of the diabatic states, and the electronic matrix element coupling the diabatic states for charge transfer transitions. These are important quantities characterizing optical and thermal charge transfer in transition metal complexes. While the two-state model is reasonably successful in interpreting the dipole-moment changes, it is less successful in predicting polarizability changes.

The measured dipole-moment changes are significantly smaller than expected and can be rationalized in terms of a model that considers the effects of electron delocalization and the shift of the valence electrons due to the change in charge distribution upon electron excitation.

Various electron-transfer distances are implicated by the dipole-moment expressions considered. As defined in Eq. (27), r^0 is the distance separating the localized donor and (reduced) acceptor charge centroids. It can be viewed as the distance between the average positions of the transferring electron and is equal to $|(\boldsymbol{\mu}_b - \boldsymbol{\mu}_a)/e|$ only if the other electrons are not affected by the charge transfer [4,22]. As shown by the modeling results, there is an appreciable contribution to $(\boldsymbol{\mu}_b - \boldsymbol{\mu}_a)$ from the shift of the ligand valence electrons, particularly for the MLCT transitions. Although the magnitude of this valence-electron shift (and the corresponding charge-centroid shift) is not large, it translates into a substantial dipole-moment change since there are many ligand valence electrons, typically > 30. In order to take the valence-electron shift into account, the effective electron-transfer distance $r_{ab} \equiv |(\boldsymbol{\mu}_b - \boldsymbol{\mu}_a)/e|$ is introduced; $|r_{ab}|$ is less than $|r^0|$ and corresponds to the distance over which a single electron would need to be transferred if its displacement were solely responsible for the dipole-moment difference between the localized states. Not only is the effective electron-transfer distance an important quantity determining dipole-moment changes in charge transfer processes, it also enters into expressions for the electronic coupling element and the solvent reorganization energy.

Acknowledgements

This research was carried out at Brookhaven National Laboratory under Contract DE-AC02-76CH00016 with the U. S. Department of Energy and supported by its Division of Chemical Sciences, Office of Basic Energy Sciences.

Appendix A. Dipole-moment contribution from electron delocalization

The reduction in the dipole moment resulting from electron delocalization in the diabatic states for the MMCT transition can be modeled as follows. For the MMCT transition in a weakly coupled mixed-valence complex such as $[(NH_3)_5Ru^{II}$–4,4′-bpy–$Ru^{III}(NH_3)_5]^{5+}$ we consider the two ruthenium centers separately, with one end modeled as $(NH_3)_5Ru^{II}L$ and the other as $LRu^{III}(NH_3)_5$. After the MMCT transition the two centers switch their identities. Considering first the Ru(II) end of the dimer, the initial state of $(NH_3)_5Ru^{II}L$ is modeled assuming that the important interaction is between the filled metal d_π and the empty ligand π^* orbital. Using an LCAO approach we can write the relevant molecular orbital as:

$$\Psi = c_a\psi_{d\pi} + c_b\psi_{L\pi^*}$$

The molecular orbital is predominately metal in character so that c_a is large and c_b small. The electronic charge on the metal center is $2c_a^2e = (2 - 2c_b^2)e$ and that on the ligand is $2c_b^2e$. Since the Ru(II) center formally has two d_π electrons and the ligand π^* orbital was empty before delocalization, the charge transferred from the metal to the ligand is $2c_b^2e$, translating to a contribution of $2c_b^2(\boldsymbol{\mu}_b - \boldsymbol{\mu}_a)$ to the ground-excited state dipole-moment change from ground-state delocalization. There is no contribution to the MLCT dipole-moment change from excited-state delocalization.

After the MMCT transition the Ru(II) end becomes $(NH_3)_5Ru^{III}L$. We assume that the important interaction is now between the half-filled metal d_π and the filled ligand π orbital. Thus, three electrons need to be considered. The relevant molecular orbitals are now:

$$\Psi_1 = c_b\psi_{d\pi} + c_a\psi_{L\pi}$$

$$\Psi_2 = -c_a\psi_{d\pi} + c_b\psi_{L\pi}$$

where Ψ_1 and Ψ_2 are the filled, lower energy and singly occupied, higher energy orbitals, respectively. Note that c_b is again the smaller coefficient. The electronic charge on the metal center is now $(2c_b^2 + c_a^2)e = (1 + c_b^2)e$. Since the Ru(III) center formally has one d_π electron (before delocalization), ligand-to-metal delocalization has increased the electronic charge on the ruthenium by c_b^2e. The corresponding contribution to the LMCT ground-excited state dipole-moment difference is $c_b^2(\boldsymbol{\mu}_b - \boldsymbol{\mu}_a)$. The delocalization present in the excited state contributes an equal, but opposite, amount to the LMCT dipole-moment change. In each case the ground-state electron delocalization is in the same direction as the corresponding MLCT or LMCT transition, with the vector for the delocalization dipole, like that of the excited-state dipole, pointing from the negative to the positive charge. Moreover, in each case electron delocalization contributes $2c_b^2(\boldsymbol{\mu}_b - \boldsymbol{\mu}_a)$ to the ground-excited state dipole-moment difference.

References

[1] W. Liptay, in: E.C. Lim (Ed.), Excited States, vol. 1, Academic Press, New York, 1974, pp. 129–229.
[2] D.H. Oh, S.G. Boxer, J. Am. Chem. Soc. 112 (1990) 8161–8162.
[3] D.H. Oh, M. Sano, S.G. Boxer, J. Am. Chem. Soc. 113 (1991) 6880–6890.
[4] Y.-g.K. Shin, B.S. Brunschwig, C. Creutz, N. Sutin, J. Phys. Chem. 100 (1996) 8157–8169.
[5] L. Karki, H.P. Lu, J.T. Hupp, J. Phys. Chem. 100 (1996) 15637–15639.
[6] M.P. de Haas, J.M. Warman, Chem. Phys. 73 (1982) 35–53.
[7] S.N. Smirnov, C.L. Braun, J. Phys. Chem. 96 (1992) 9587–9591.
[8] S.N. Smirnov, C.L. Braun, J. Phys. Chem. 98 (1994) 1953–1961.
[9] S.N. Smirnov, C.L. Braun, Chem. Phys. Lett. 217 (1994) 167–172.
[10] R.W. Fessenden, A. Hitachi, J. Phys. Chem. 91 (1987) 3456–3462.
[11] J.C. Curtis, B.P. Sullivan, T.J. Meyer, Inorg. Chem. 22 (1983) 224–236.
[12] C. Creutz, M.H. Chou, Inorg. Chem. 26 (1987) 2995–3000.
[13] J.R. Schoonover, K.G. Gordon, R. Argazzi, W.H. Woodruff, K.A. Peterson, C.A. Bignozzi, et al., J. Am. Chem. Soc. 115 (1993) 10996–10997.
[14] H. Lu, V. Petrov, J.T. Hupp, Chem. Phys. Lett. 235 (1995) 521–527.
[15] J.R. Reimers, N.S. Hush, J. Phys. Chem. 95 (1991) 9773–9781.
[16] J.R. Reimers, N.S. Hush, in: K. Prassides (Ed.), Mixed Valency Systems: Applications in Chemistry, Physics and Biology, Kluwer Academic Publishers, Dordrecht, 1991, pp. 29–50.
[17] Y.-g. K. Shin, B.S. Brunschwig, C. Creutz, N. Sutin, J. Am. Chem. Soc. 117 (1995) 8668–8669.
[18] L. Karki, J.T. Hupp, J. Am. Chem. Soc. 119 (1997) 4070–4073.
[19] H. Labhart, Adv. Chem. Phys. 13 (1967) 179–204.
[20] W. Baumann, in: B.W. Rossiter, J.F. Hamilton (Eds.), Physical Methods of Chemistry, vol. IIIB, Wiley, New York, 1989, pp. 45–131.
[21] W. Baumann, Z. Nagy, A.K. Maiti, H. Reis, S.V. Rodriques, N. Detzer, in: N. Mataga, T. Okada, H. Masuhara (Eds.), Dynamics and Mechanism of Photoinduced Charge Transfer and Related Phenomena, Elsevier, Amsterdam, 1992, pp. 211–229.
[22] C. Creutz, M.D. Newton, N. Sutin, J. Photochem. Photobiol. A: Chem. 82 (1994) 47–59.
[23] R.J. Cave, M.D. Newton, Chem. Phys. Lett. 249 (1996) 15–19.
[24] R.H. Magnuson, H. Taube, J. Am. Chem. Soc. 97 (1975) 5129–5136.
[25] Y.-g. K. Shin, B.S. Brunschwig, C. Creutz, M.D. Newton, N. Sutin, J. Phys. Chem. 100 (1996) 1104–1110.
[26] L. Karki, J.T. Hupp, Inorg. Chem. 36 (1997) 3318–3321.
[27] D.H. Oh, S.G. Boxer, J. Am. Chem. Soc. 111 (1989) 1130–1131.
[28] C. Turro, Y.C. Chung, N. Leventis, M.E. Kuchenmeister, P.J. Wagner, G.E. Leroi, Inorg. Chem. 35 (1996) 5104–5106.
[29] M. Zerner, ZINDO Quantum Chemistry Package, University of Florida.
[30] J. Zeng, N.S. Hush, J.R. Reimers, J. Phys. Chem. 100 (1996) 19292–19294.
[31] J. Zeng, N.S. Hush, J.R. Reimers, J. Am. Chem. Soc. 118 (1996) 2059–2068.
[32] C. Creutz, Prog. Inorg. Chem. 30 (1983) 1–73.
[33] D.K. Lavallee, E.B. Fleischer, J. Am. Chem. Soc. 94 (1972) 2583–2599.
[34] D.K. Lavallee, E.B. Fleischer, J. Am. Chem. Soc. 94 (1972) 2599–2601.
[35] J.E. Sutton, H. Taube, Inorg. Chem. 20 (1981) 4021–4023.
[36] C.M. Elliot, D.L. Derr, S. Ferrere, M.D. Newton, Y.-P. Liu, J. Am. Chem. Soc. 118 (1996) 5221–5228.
[37] R.S. Mulliken, W.B. Person, Molecular Complexes, Wiley, New York, 1969.
[38] Y.-g. K. Shin, D.J. Szalda, B.S. Brunschwig, C. Creutz, N. Sutin, Inorg. Chem. 36 (1997) 4001–4007.
[39] B.S. Brunschwig, S. Ehrenson, N. Sutin, J. Phys. Chem. 90 (1986) 3657–3668.
[40] P. Forlano, L.M. Baraldo, J.A. Olabe, C.O. Della Vedova, Inorg. Chim. Acta 223 (1994) 37–42.
[41] B.S. Brunschwig, N. Sutin, Coord. Chem. Rev. (in press).